Ylangene-Type and Nardosinane-Type Sesquiterpenoids from the Soft Corals *Lemnalia flava* and *Paralemnalia thyrsoides*

Shi-Yie Cheng,[a,b] En-Hung Lin,[a] Jing-Shi Huang,[a] Zhi-Hong Wen,[a,b] and Chang-Yih Duh*,[a,b]

[a] *Department of Marine Biotechnology and Resources, National Sun Yat-sen University; and* [b] *Asia-Pacific Ocean Research Center, National Sun Yat-sen University; Kaohsiung 80424, Taiwan.*

Received November 12, 2009; accepted December 16, 2009; published online December 17, 2009

Chemical investigations of the Formosan soft coral *Lemnalia flava* have obtained a new ylangene-type sesquiterpenoid, (1*S*,2*S*,4*R*,6*S*,7*R*,8*S*)-4α-formyloxy-β-ylangene (1), along with two known sesquiterpenoids, lemnalol (2) and isolemnalol (3). Three new nardosinane-type sesquiterpenoids, designated as paralemnolins J—L (4—6), and five known sesquiterpenoids (7—11), were isolated from the other soft coral *Paralemnalia thyrsoides*. The structures of metabolites 1 and 4—6 were elucidated through extensive spectroscopic analysis and chemical methods. Moreover, the anti-inflammatory activity of metabolites 1—7 and 11 was evaluated *in vitro*.

Key words *Lemnalia flava*; ylangene-type sesquiterpenoid; nardosinane-type sesquiterpenoid; *Paralemnalia thyrsoides*; anti-inflammatory activity

Sesquiterpenoids, norsesquiterpenoids, and their analogues, especially those of the genera *Lemnalia* and *Paralemnalia*, constitute a large family of secondary metabolites endowed with a wide range of structural diversity.[1—18] Previous bioassay results of these secondary metabolites have been shown to exhibit diverse biological properties such as cytotoxic,[5,7,9—11,16] anti-inflammatory[12] and antibacterial activities.[16] As part of continuing search for bioactive secondary metabolites from marine invertebrates, we investigated the secondary metabolites of the Formosan soft corals *Lemnalia flava* and *Paralemnalia thyrsoides*.

A new ylangene-type sesquiterpenoid, (1*S*,2*S*,4*R*,6*S*,7*R*,8*S*)-4α-formyloxy-β-ylangene (**1**) (Fig. 1), along with two known ylangene-type sesquiterpenoids, lemnalol (**2**)[10] and isolemnalol (**3**),[7] were isolated from the Formosan soft coral *L. flava*. In addition, chemical investigations of the other Formosan soft coral *P. thyrsoides* have obtained three new nardosinane-type sesquiterpenoids, paralemnolins J—L (**4**—**6**) (Fig. 1), and five previously characterized sesquiterpenoids (**7**—**11**).[11,17,19] The details of isolation and structural elucidation of metabolites **1** and **4**—**6** are discussed in this paper. Moreover, metabolite **2** (10 μM) was evaluated for the ability to inhibit the expression of the pro-inflammatory iNOS (inducible nitric oxide synthase) and COX-2 (cyclooxygenase-2) proteins. Metabolites **1** and **11** did not inhibit the COX-2 protein expression, but significantly inhibited iNOS protein expression. However, metabolites **3**—**7** showed insignificantly anti-inflammatory activity against LPS (lipopolysaccharide)-stimulated RAW 264.7 macrophages.

Results and Discussion

The chromatographic separation of the EtOAc extracts of the Formosan soft corals *L. flava* and *P. thyrsoides* using Si 60, RP-18, and Sephadex LH-20 gravity columns in combination with RP-18 HPLC resulted in the purification of metabolites **1**—**11** (see Experimental).

(1*S*,2*S*,4*R*,6*S*,7*R*,8*S*)-4α-Formyloxy-β-ylangene (**1**) was obtained as a yellow oil. The HR-electrospray ionization (ESI)-MS of **1** exhibited a pseudomolecular ion peak at *m*/*z* 271.1675 $[M+Na]^+$, consistent with the molecular formula of $C_{16}H_{24}O_2$, requiring five degrees of unsaturation. The presence of an *exo*-methylene moiety was indicated by its NMR data (Tables 1, 2) [δ_H 5.09 (1H, s, H-12a) and 4.95 (1H, s, H-12b); δ_C 115.0 (CH_2, C-12) and 148.8 (qC, C-3)]. The ^{13}C-NMR data also showed signals of three methyl carbons [δ_C 19.5 (CH_3, C-11), 20.0 (CH_3, C-14), and 20.2 (CH_3, C-15)], three sp^3 methylene carbons [δ_C 32.4 (CH_2, C-5), 21.6 (CH_2, C-9), and 36.4 (CH_2, C-10)], five sp^3 methine carbons [δ_C 47.4 (CH, C-2), 68.4 (CH, C-4), 47.1 (CH, C-6), 41.8 (CH, C-7), and 32.4 (CH, C-13)], and one sp^3 quaternary carbon [δ_C 42.6 (qC, C-1)]. The ^{1}H-NMR spectrum of **1** showed signals due to a tertiary methyl at δ_H 0.67 (3H, s, Me-11) and an isopropyl group at δ_H 0.88 (6H, d, J=6.3 Hz, Me-14 and Me-15) and 1.52 (1H, m, H-13) in addition to the signals at δ_H 1.81 (1H, dd, J=15.3, 3.6 Hz, H-5α), 2.43 (1H, dd, J=15.3, 8.1 Hz, H-5β), 2.61 (1H, d, J=5.9 Hz, H-2), and 2.13 (1H, s,

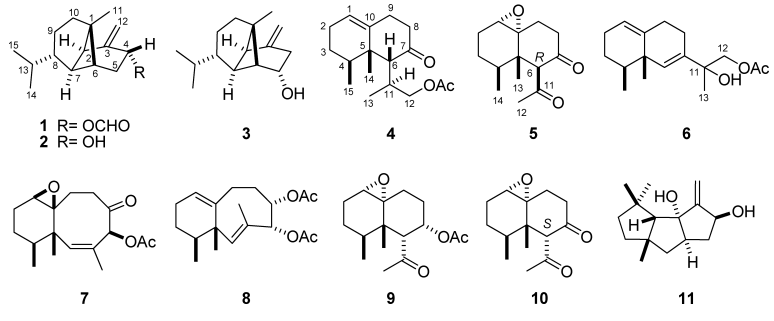

Fig. 1. Structures of Metabolites **1**—**11**

* To whom correspondence should be addressed. e-mail: yihduh@mail.nsysu.edu.tw

Table 1. ^{1}H-NMR Spectroscopic Data of Metabolites **1** and **4**—**6**

H#	**1**[a]	**4**[a]	**5**[b]	**6**[a]
1		5.58 br d (4.8)[c]	3.19 d (4.0)[c]	5.37 br s
2	2.61 d (5.9)[c]	α: 2.03 m; β: 2.15 m	α: 1.98 m; β: 2.00 m	2.00 m
3		α: 1.45 m; β: 1.49 m	α: 1.19 m; β: 1.26 m	α: 2.17 m; β: 2.30 m
4	5.64 br d (8.1)	2.11 m	1.98 m	1.48 m
5	α: 1.81 dd (15.3, 3.6)			
	β: 2.43 dd (15.3, 8.1)			
6	1.58 m	2.37 m	3.77 m	5.83 s
7	2.13 s			
8	1.54 m	α: 2.43 m; β: 2.38 m	α: 2.82 m; β: 2.50 m	1.50 m
9	1.62 m	α: 2.50 m; β: 2.67 m	α: 2.50 m; β: 1.40 m	α: 2.00 m; β: 2.17 m
10	1.71 m			
11	0.67 s	2.19 m		
12	a: 5.09 s	a: 3.70 t (10.4)	2.23 s	a: 3.99 d (11.2)
	b: 4.95 s	b: 4.53 dd (10.4, 2.9)		b: 4.12 d (11.2)
13	1.52 m	0.95 d (6.8)	2.14 s	1.30 s
14	0.88 d (6.3)	0.92 s	0.68 d (6.5)	0.94 s
15	0.88 d (6.3)	0.83 d (6.8)		0.95 d (6.8)
4-OC<u>H</u>O	8.10 s			
12-OAc		2.03 s		2.07 s

a) Spectra were measured in $CDCl_3$ (300 MHz). *b*) Spectra were measured in $CDCl_3$ (500 MHz). *c*) *J* values (in Hz) are in parentheses.

Table 2. ^{13}C-NMR Spectroscopic Data of Metabolites **1** and **4**—**6**

C#	**1**[a]	**4**[a]	**5**[b]	**6**[a]
1	42.6 (qC)[c]	124.1 (CH)[c]	62.1 (CH)[c]	119.9 (CH)[c]
2	47.4 (CH)	25.8 (CH_2)	22.5 (CH_2)	25.3 (CH_2)
3	148.8 (qC)	26.9 (CH_2)	25.7 (CH_2)	29.9 (CH_2)
4	68.4 (CH)	33.1 (CH)	34.3 (CH)	37.4 (CH)
5	32.4 (CH_2)	43.0 (qC)	45.3 (qC)	38.1 (qC)
6	47.1 (CH)	62.2 (CH)	69.4 (CH)	129.7 (CH)
7	41.8 (CH)	213.1 (qC)	206.3 (qC)	137.8 (qC)
8	44.2 (qC)	40.7 (CH_2)	38.7 (CH_2)	27.3 (CH_2)
9	21.6 (CH_2)	30.8 (CH_2)	30.2 (CH_2)	27.6 (CH_2)
10	36.4 (CH_2)	137.8 (qC)	65.3 (qC)	141.9 (qC)
11	19.5 (CH_3)	31.6 (CH)	207.6 (qC)	73.9 (qC)
12	115.0 (CH_2)	66.3 (CH_2)	34.2 (CH_3)	70.1 (CH_2)
13	32.4 (CH)	17.9 (CH_3)	14.4 (CH_3)	24.2 (CH_3)
14	20.0 (CH_3)	21.8 (CH_3)	18.3 (CH_3)	15.7 (CH_3)
15	20.2 (CH_3)	15.3 (CH_3)		20.9 (CH_3)
4-OC<u>H</u>O	160.7 (CH)			
12-OAc		20.9 (CH_3)		20.7 (CH_3)
		170.9 (qC)		171.1 (qC)

a) Spectra were measured in $CDCl_3$ (75 MHz). *b*) Spectra were measured in $CDCl_3$ (125 MHz). *c*) Multiplicities are deduced by HSQC and DEPT experiments.

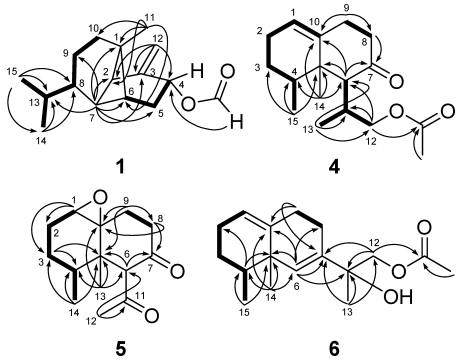

Fig. 2. Selected ^{1}H–^{1}H COSY (—) and HMBC (→) Correlations of **1** and **4**—**6**

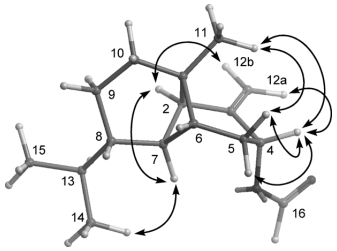

Fig. 3. Key NOESY Correlations of **1**

H-7). These NMR features were analogous to those of **2**[10] with the exception that the resonances due to the secondary hydroxyl [δ_H 4.42 (1H, br d, J=8.0 Hz, H-4); δ_C 66.5 (CH, C-4)] were replaced by a secondary formyloxyl [δ_H 5.64 (1H, br d, J=8.1 Hz, H-4), 8.10 (1H, s, H-16); δ_C 68.4 (CH, C-4) and 160.7 (CH, C-16)]. This assumption was further supported by its IR spectrum absorptions at 2853 and 1724 cm^{-1}. Moreover, the ^{1}H–^{1}H correlation spectroscopy (COSY) correlations (Fig. 2) between H-4 and H-16, and the heteronuclear multiple bond correlation (HMBC) correlations from H-16 to C-4 confirmed the location of the formyloxy functionality at C-4. Therefore, the planar structure of **1** was proposed decidedly.

The computer modeled 3D structure of **1** was generated by using MM2 force field calculations for energy minimization with the molecular modeling program Chem3D Ultra 9.0. The relative stereochemistry of **1** assigned by the nuclear Overhauser effect spectroscopy (NOESY) spectrum was compatible with those of **1** offered by computer modeling, in which the close contacts of atoms calculated in space were consistent with the NOESY correlations (Fig. 3). A large long-range coupling constant ($^4J_{2,6}$=5.9 Hz) due to a W-type coupling between H-2 and H-6 further indicated the presence of a bridged cyclobutane system in **1**. In addition, no coupling was observed between H-7 and the adjacent protons (H-2, H-6, and H-8), suggesting a dihedral angle of approximately 90° between these protons. The NOESY correlations between H_3-11 with both H-4 and H-5β positioned the β-orientation of the aforementioned protons. Furthermore, H-7

was found to show the NOE correlations with both H-2 and H_3-14, indicating the α-orientations of H-2, H-7, and the isopropyl group.

In order to determine the absolute stereochemistry, metabolite **1** was hydrolyzed with K_2CO_3/MeOH to give a hydrolyte **1a**.[20] By a careful comparison of NMR spectroscopic data, the ^{1}H- and ^{13}C-NMR data of **1a** were in good agreement with those of lemnalol (**2**).[10] The absolute stereochemistry of **1a** was further elucidated by comparison of its optical rotation ($[\alpha]_D^{24}$ −8.9) with that of **2** ($[\alpha]_D^{20}$ −9.3). On the basis of the above observations, together with NOESY correlations (Fig. 3), metabolite **1** was determined to be (1*S*,2*S*,4*R*,6*S*,7*R*,8*S*)-4α-formyloxy-β-ylangene.

The positive HR-ESI-MS of **4** exhibited a pseudomolecular ion peak at *m*/*z* 301.1781 $[M+Na]^+$, corresponding to the molecular formula $C_{17}H_{26}O_3$ and five degrees of unsaturation. The NMR spectroscopic data (Tables 1, 2) demonstrated the presences of a keto group, an acetate unit, and a trisubstituted double bond, which accounted for three degrees of five unsaturations and were suggestive of a bicyclic decalin ring. The assignment of the keto carbonyl signal at δ_C 213.1 (C-7) was clarified by analysis of the key HMBC correlations from H-6 to C-7 and from H_2-8 to C-7 (Fig. 2). One acetate resonated at δ_H 2.03 (each 3H, s) and δ_C 170.9 (qC) and 20.9 (CH_3). Meanwhile, the oxymethylene at δ_H 3.70 (H-12a) and 4.53 (H-12b) exhibited the HMBC correlations to the acetoxy carbonyl, proving acetyloxy substitution at the position, and was confirmed by the COSY correlations (Fig. 2). The HMBC correlations from the methyl signal (H_3-14) correlated with those of two methine carbons (C-4 and C-6), a quaternary carbon (C-5), and a quaternary olefinic carbon (C-10) as well as COSY correlations from H_2-8 to H_2-9, led to the placement of the trisubstituted double bond at C-1 and C-10. On the basis of the key COSY and HMBC correlations (Fig. 2), metabolite **4** was fully assigned as a decalin ring belonging to the nardosinane-type sesquiterpenoid.

The relative configuration of **4** was proposed on the basis of the key NOESY correlations (Fig. 4). The NOESY correlations between H-2β/H_3-14, H-9β/H_3-14, H-2β/H_3-15, H-6/H_3-14, H-6/H_3-15, H-6/H_3-13, H_3-14/H_3-15, H-4/H-2α, and H-4/H-11 showed that H-6, H_3-14, and H_3-15 are located on β face of the decalin ring, whereas H-4 and H-2α are oriented toward the opposite face. The above findings also confirmed the 4*S**, 5*S**, and 6*R** configurations. Moreover, H-12a showed a crucial NOESY correlation with H-8α, allowing the *S**-configuration of the C-11. According to the aforementioned observations, the structure of paralemnolin J (**4**) was proposed unambiguously.

Paralemnolin K (**5**) was isolated as a colorless oil, which analyzed for the molecular formula $C_{14}H_{20}O_3$ by HR-ESI-MS coupled with the distortionless enhancement by polarization transfer (DEPT) and ^{13}C-NMR spectroscopic data (Table 2). Metabolite **5** was found to possess the same molecular formula as that of **10**[17] ($C_{14}H_{20}O_3$), as revealed from HR-ESI-MS. The above result, together with the comparison of 2D NMR spectroscopic data of **5** with those of **10**, disclosed that two metabolites had isomeric relationship. The significant proton and carbon chemical shift differences between **5** and **10** demonstrated that the relative configuration at C-6 of **5** possessed the *R*-configuration. The key NOESY correlations between H_3-13/H_3-14, H_3-14/H-3β, H-1/H-9β, H-8β/H-9β, and H_3-13/H-8β positioned the β-orientation of the aforementioned protons. Furthermore, H-4 was found to show the NOESY correlations with both H-3α and H-6, suggesting the α-orientations of H-4 and H-6. The above findings indicated the 1*S**, 4*S**, 5*S**, 6*R**, and 10*R** configurations. Consequently, the structure of paralemnolin K (**5**) was determined undoubtedly.

The HR-ESI-MS of metabolite **6**, appeared as a colorless oil, established a molecular formula of $C_{17}H_{26}O_3$, implying five degrees of unsaturation. Analysis of the COSY and HMBC correlations (Fig. 2) were diagnostic in determining that the gross framework of paralemnolin L, possessing a nardosinane-type sesquiterpene skeleton, was assigned as **6**. The structure of **6** was identical to that of paralemnolin C[15] with exception that the acetoxy group attached to C-11 was replaced by a hydroxy group. A tertiary hydroxyl was recognized as being present in **6** from its ^{13}C-NMR signals at δ_C 73.9 (qC, C-11), as well as from a broad IR absorption at 3459 cm^{-1}. The NOESY correlations between H_3-14 and H_3-15 implied these protons were located on the same face (β-orientation) of the decalin ring in the molecule of **6**. The result indicated that **6** possessed the same stereochemistry as paralemnolin C at each ring junction and chiral center. On the basis of these evidences, the structure of paralemnolin L (**6**) was confirmed definitely.

Due to previous reports of iNOS (inducible nitric oxide synthetase) and COX-2 (cyclooxygenase-2) inhibition activity of Alcyonaceous sesquiterpenoids,[21,22] we evaluated the anti-inflammatory activity of these isolated metabolites. The *in vitro* anti-inflammatory effects of **1**—**7** and **11** were tested using LPS-stimulated cells. Stimulation of RAW 264.7 macrophage cells with LPS resulted in up-regulation of the pro-inflammatory iNOS and COX-2 proteins. Metabolites **1**—**7** and **11** (10 μM) reduced the levels of the iNOS protein (70.0±7.0%, 2.0±0.8%, 103.0±4.3%, 110.6±1.8%, 110.1±3.3%, 132.5±4.2%, 216.9±5.1%, and 13.1±2.1%, respectively) and COX-2 protein (108.3±0.9%, 25.0±6.7%, 94.3±3.2%, 116.9±8.3%, 113.6±2.7%, 121.7±3.8%, 152.3±5.6%, and 67.6±13.1%, respectively) compare with the control cells (LPS alone). The primary anti-inflammatory results showed that **2** and **11** significantly inhibited iNOS and COX-2 proteins expression. Metabolites **1** did not inhibit the COX-2 protein expression, but significantly inhibited iNOS protein expression. With the exception of the above findings, the obtained negative results showed that **3**—**7** exhibited no discernible anti-inflammatory activity against LPS-stimulated RAW 264.7 macrophages. Moreover, the housekeeping protein β-actin was not changed by the presence of these tested metabolites at the same concentration. Under the same experimental conditions, 10 μM CAPE (caffeic acid phenylthyl

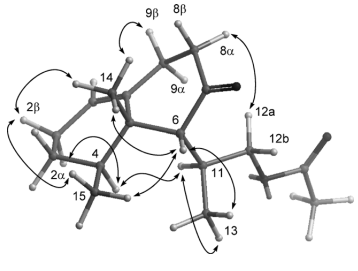

Fig. 4. Key NOESY Correlations of **4**

ester) reduced the levels of the iNOS and COX-2 protein to 1.5±2.1% and 70.2±11.5%, respectively, relative to the control cells stimulated with LPS.

Experimental

General Experimental Procedures Optical rotations were determined with a JASCO P1020 digital polarimeter. IR spectra were recorded on a JASCO FT/IR-4100 infrared spectrophotometer. UV spectra were obtained on a JASCO V-650 spectrophotometer. The NMR spectra were recorded on a Bruker Advance 300 NMR spectrometer at 300 MHz for ^{1}H and 75 MHz for ^{13}C or on a Varian Unity INOVA 500 FT-NMR spectrometer at 500 MHz for ^{1}H and 125 MHz for ^{13}C, respectively, using $CDCl_3$ with tetramethylsilane (TMS) as internal standard. Chemical shifts are given in δ (ppm) and coupling constants in Hz. ESI-MS were recorded by ESI FT-MS on a Bruker APEX II mass spectrometer. Silica gel 60 (Merck, 230—400 mesh) and Sephadex LH-20 (Pharmacia) were used for column chromatography. Precoated silica gel plates (Merck, Kieselgel 60 F_{254}, 0.25 mm) were used for TLC analyses. High-performance liquid chromatography (HPLC) was carried out using a Hitachi L-7100 pump equipped with a Hitachi L-7400 UV detector at 220 nm and a semi-preparative reversed-phase column (Merck, Hibar Purospher RP-18e, 5 μm, 250×10 mm).

Animal Material The Formosan soft corals *L. flava* and *P. thyrsoides* were collected by hand using scuba at the Green Islands located in the southeast coast of Taiwan, in July 2005, at a depth of 10 m, and was stored in a freezer for 5 weeks until extraction. Both specimens were identified by one of the authors (C.-F. D.), and voucher specimens (GN-76 and GN-78) were deposited in the Department of Marine Biotechnology and Resources, National Sun Yat-sen University.

Extraction and Isolation The frozen soft coral *L. flava* was chopped into small pieces and extracted with acetone for 24 h at room temperature. The quantity of solvent used for each extraction (2.0 l) was at least three times the amount of the soft coral material used (1.2 kg). The combined extracts were concentrated *in vacuo* (under 35 °C) to obtain 35.0 g of dry extract, which was suspended in water and extracted with EtOAc and *n*-BuOH (saturated with H_2O) sequentially. The EtOAc phase was evaporated to dryness *in vacuo* to give a dark brown residue (25 g). The resulting EtOAc residue was chromatographed over Si gel 60 using *n*-hexane, *n*-hexane–EtOAc and EtOAc–MeOH mixtures of increasing polarity as eluting solvent to obtain 30 fractions. Fraction 9 (1.2 g) derived from the *n*-hexane–EtOAc (90 : 10) elution was subjected to a silica gel column using *n*-hexane–EtOAc (95 : 5) for elution to afford **1** (30 mg). Fraction 10 (4.5 g) eluted from *n*-hexane–EtOAc (90 : 10) was subjected to a silica gel column using *n*-hexane–EtOAc (95 : 5) as eluting solvent to afford **2** (3.0 g). Fraction 12 (0.8 g) derived from the *n*-hexane–EtOAc (90 : 10) elution was subjected to a silica gel column using *n*-hexane–EtOAc mixtures of increasing polarity for elution, to afford 10 subfractions. A subfraction 12-3 (240 mg) eluted by *n*-hexane–EtOAc (95 : 5) was fractionated over Sephadex LH-20 column eluting with CH_2Cl_2–MeOH (1 : 1) to produce a mixture (78 mg) that was further purified by HPLC (RP-18) using 85% MeOH in H_2O as eluent to give **3** (5 mg).

In the same manner, the EtOAc fraction (10.0 g) of the other soft coral *P. thyrsoides* was subjected to gravity column chromatography on silica gel 60 to furnish 28 fractions. Fraction 12 (1.2 g) obtained from the *n*-hexane–EtOAc (30 : 1) elution was subjected to a silica gel 60 column using *n*-hexane–acetone mixtures of increasing polarity for elution, to afford 10 subfractions. A subfraction 12-5 (74 mg) eluted with *n*-hexane–acetone (35 : 1) was fractionated over Sephadex LH-20 gel using acetone as eluent to affford **7** (2 mg). In turn, a subfraction 12-6 (160 mg) eluted with *n*-hexane–acetone (30 : 1) was applied to Sephadex LH-20 to afford a mixture containing **4** and **8**. Metabolite **4** (16 mg) and **8** (2 mg) were further purified by RP-18 HPLC eluting with MeOH–H_2O (19 : 1). Similarly, metabolite **6** (5 mg) was obtained by a Sephadex LH-20 column on fraction 17. Fraction 22 (265 mg) eluted with *n*-hexane–EtOAc (10 : 1) was submitted to repeated chromatography over silica gel using *n*-hexane–EtOAc mixtures of increasing polarity as eluent, to yield a mixture (124 mg), which was further purified by RP-18 HPLC eluting with 90% MeOH in H_2O (flow rate 5.0 ml/min) to afford **5** (2 mg), **9** (3 mg), and **10** (20 mg). Fraction 24 (174 mg) eluted from *n*-hexane–acetone (10 : 1) was fractionated over Sephadex LH-20 eluting with CH_2Cl_2–MeOH (1 : 1) to produce **11** (18 mg).

(1*S*,2*S*,4*R*,6*S*,7*R*,8*S*)-4α-Formyloxy-β-ylangene (**1**): Light yellow, viscous oil; $[\alpha]_D^{25}$ −47 (c=0.3, CH_2Cl_2); IR (KBr) ν_{max} 2926, 2853, 1724, 1174, 906 cm^{-1}; ^{1}H-NMR ($CDCl_3$, 300 MHz) and ^{13}C-NMR ($CDCl_3$, 75 MHz) spectroscopic data, see Tables 1 and 2; ESI-MS *m*/*z*: 271 $[M+Na]^+$; HR-ESI-MS *m*/*z*: 271.1675 $[M+Na]^+$ (Calcd for $C_{16}H_{24}O_2Na$, 271.1674).

Paralemnolin J (**4**): Colorless, viscous oil; $[\alpha]_D^{25}$ −59 (c=0.2, CH_2Cl_2); IR (KBr) ν_{max} 2926, 1734, 1442, 1240, 1067, 1021 cm^{-1}; ^{1}H-NMR ($CDCl_3$, 300 MHz) and ^{13}C-NMR ($CDCl_3$, 75 MHz) spectroscopic data, see Tables 1 and 2; ESI-MS *m*/*z*: 301 $[M+Na]^+$; HR-ESI-MS *m*/*z*: 301.1781 $[M+Na]^+$ (Calcd for $C_{17}H_{26}O_3Na$, 301.1780).

Paralemnolin K (**5**): Colorless, viscous oil; $[\alpha]_D^{25}$ −33 (c=0.2, CH_2Cl_2); IR (KBr) ν_{max} 2924, 1717, 1612, 1443, 1203, 1079 cm^{-1}; ^{1}H-NMR ($CDCl_3$, 500 MHz) and ^{13}C-NMR ($CDCl_3$, 125 MHz) spectroscopic data, see Tables 1 and 2; ESI-MS *m*/*z*: 259 $[M+Na]^+$; HR-ESI-MS *m*/*z*: 259.1311 $[M+Na]^+$ (Calcd for $C_{14}H_{20}O_3Na$, 259.1310).

Paralemnolin L (**6**): Colorless, viscous oil; $[\alpha]_D^{25}$ +100 (c=0.2, CH_2Cl_2); IR (KBr) ν_{max} 3459, 2925, 1737, 1615, 1443, 1219, 1094, 775 cm^{-1}; ^{1}H-NMR ($CDCl_3$, 300 MHz) and ^{13}C-NMR ($CDCl_3$, 75 MHz) spectroscopic data, see Tables 1 and 2; ESI-MS *m*/*z*: 301 $[M+Na]^+$; HR-ESI-MS *m*/*z*: 301.1781 $[M+Na]^+$ (Calcd for $C_{17}H_{26}O_3Na$, 301.1780).

Hydrolysis of 1 with K_2CO_3/MeOH To a solution of K_2CO_3 (5.0 mg) in 3 ml anhydrous MeOH was added **1** (6.0 mg). The mixture was stirred for overnight at room temperature. The mixture was diluted with EtOAc, washed with 1 N HCl brine, and dried over $MgSO_4$. The crude product was then subjected to a short silica-gel column using *n*-hexane–EtOAc (9 : 1) as eluent to afford **1a** (4.0 mg). By a careful comparison of physical and NMR spectroscopic data, the ^{1}H- and ^{13}C-NMR, and optical rotation data of **1a** were in good agreement with those of lemnalol (**2**).[10]

***In Vitro* Anti-inflammatory Assay** Murine RAW 264.7 macrophages were obtained from the American Type Culture Collection (ATCC, No. TIB-71) and cultured in Dulbecco's modified essential medium (DMEM) containing 10% heat-inactivated fetal bovine serum, at 37 °C in a humidified 5% CO_2–95% air incubator under standard conditions. The *in vitro* anti-inflammatory assay was carried out according to the procedure described previously.[22—24] For statistical analysis, all the data were analyzed by a one-way analysis of variance (ANOVA), followed by the Student–Newman–Keuls *post hoc* test for multiple comparisons. A significant difference was defined as a p value of <0.05.

Acknowledgments This work was financially supported by grants from the National Science Council (NSC96-2320-B-110-003-MY3) of the Republic of China (Taiwan) awarded to C.-Y. D.

References and Notes

1) Blunt J. W., Copp B. R., Hu W.-P., Munro M. H. G., Northcote P. T., Prinsep M. R., *Nat. Prod. Rep.*, **26**, 170—244 (2009), and literature cited in previous reviews.
2) Tursch B., Braekman J. C., Daloze D., Fritz P., Kelecom A., Karlsson R., Losman D., *Tetrahedron Lett.*, **9**, 747—750 (1974).
3) Izac R. R., Fenical W., Tagle B., Clardy J., *Tetrahedron*, **37**, 2569—2573 (1981).
4) Carney J. R., Pham A. T., Yoshida W. Y., Scheuer P. J., *Tetrahedron Lett.*, **33**, 7115—7118 (1992).
5) Jurek J., Scheuer P. J., *J. Nat. Prod.*, **56**, 508—513 (1993).
6) Bowden B. F., Coll J. C., Engelhardt L. M., Tapiolas D. M., White A. H., *Aust. J. Chem.*. **39**, 103—121 (1986).
7) Duh C.-Y., El-Gamal A. A. H., Song P.-Y., Wang S.-K., Dai C.-F., *J. Nat. Prod.*, **67**, 1650—1653 (2004).
8) Bowden B. F., Coll J. C., Mitchell S. J., *Aust. J. Chem.*, **33**, 681—684 (1980).
9) El-Gamal A. A. H., Chiu E.-P., Li C.-H., Cheng S.-Y., Dai C.-F., Duh C.-Y., *J. Nat. Prod.*, **68**, 1749—1753 (2005).
10) Kikuchi H., Tsukitani Y., Yamada Y., Iguchi K., Drexler S. A., Clardy J., *Tetrahedron Lett.*, **23**, 1063—1066 (1982).
11) Huang H.-C., Chao C.-H., Su J.-H., Hsu C.-H., Chen S.-P., Kuo Y.-H., Sheu J.-H., *Chem. Pharm. Bull.*, **55**, 876—880 (2007).
12) Huang H.-C., Wen Z.-H., Chao C.-H., Ahmed A. F., Chiang M. Y., Kuo Y.-H., Hsu C.-H., Sheu J.-H., *Tetrahedron Lett.*, **47**, 8751—8755 (2006).
13) Bishara A., Yeffet D., Sisso M., Shmul G., Schleyer M., Benayahu Y., Rudi A., Kashman Y., *J. Nat. Prod.*, **71**, 375—380 (2008).
14) Su J.-Y., Zhong Y.-L., Zeng L.-M., *J. Nat. Prod.*, **56**, 288—291 (1993).
15) Huang H.-C., Chao C.-H., Liao J.-H., Chiang M. Y., Dai C.-F., Wu Y.-C., Sheu J.-H., *Tetrahedron Lett.*, **46**, 7711—7714 (2005).
16) Yao G., Vidor N. B., Foss A. P., Chang L. C., *J. Nat. Prod.*, **70**, 901—905 (2007).
17) Izac R. R., Schneider P., Swain M., Fenical W., *Tetrahedron Lett.*, **23**, 817—820 (1982).

18) Bowden B. F., Coll J. C., Mitchell S. J., Nemorin L. E., Sternhell S., *Tetrahedron Lett.*, **21**, 3105—3108 (1980).
19) Sheikh Y. M., Singy G., Kaisin M., Eggert H., Djerassi C., Tursch B., Daloze D., Braekman J. C., *Tetrahedron*, **32**, 1171—1178 (1976).
20) Tanyeli C., Demir A. S., Dikici E., *Tetrahedron: Asymmetry*, **7**, 2399—2402 (1996).
21) Cheng S.-Y., Huang Y.-C., Wen Z.-H., Chiou S.-F., Wang S.-K., Hsu C.-H., Dai C.-F., Duh C.-Y., *Tetrahedron Lett.*, **50**, 802—806 (2009).
22) Jean Y.-H., Chen W.-F., Sung C.-S., Duh C.-Y., Huang S.-Y., Lin C.-S., Tai M.-H., Wen Z.-H., *Br. J. Pharmacol.*, **158**, 713—725 (2009).
23) Cheng S.-Y., Wen Z.-H., Chiou S.-F., Hsu C.-H., Wang S.-K., Dai C.-F., Chiang M. Y., Duh C.-Y., *Tetrahedron*, **64**, 9698—9704 (2008).
24) Cheng S.-Y., Wen Z.-H., Wang S.-K., Chiou S.-F., Hsu C.-H., Dai C.-F., Duh C.-Y., *Bioorg. Med. Chem.*, **17**, 3763—3769 (2009).